Quasi-Synchronous Code-Division Multiple Access with High-Order Modulation

Wim J. van Houtum, *Member, IEEE*

***Abstract*—Code-division multiple access (CDMA) is a multiplexing technique where a number of users simultaneously access a transmission channel by modulating and spreading their signals with preassigned codewords. This paper studies the performance of CDMA signals with orthogonal (Walsh–Hadamard) codewords and synchronization errors smaller than the chip time. Two high-order modulation techniques, M-level quadrature amplitude modulation (M-QAM) and M-level phase-shift keying (M-PSK) are compared with respect to bit-error rate (BER). The results are especially important for the return channel of cable TV networks and summarized as follows.**

- **Synchronization errors between transmitters lead to interference noise, whereas synchronization errors between the transmitter and the receiver lead to a decreased amplitude of the received user signal. Both effects have significant impact on the system performance.**
- **Closed expressions are obtained for the BER of a CDMA signal with M-PSK and M-QAM with a given maximum synchronization error.**
- **The higher the modulation order, the more sensitive the system gets for synchronization errors.**
- **The BER is highly dependent on the assigned codewords out of the Walsh–Hadamard code set.**
- **The BER performance of M-QAM outperforms that of M-PSK.**

***Index Terms*—CDMA, digital communication, high-order modulation, spread spectrum, Walsh–Hadamard codewords.**

I. Introduction

CODE-DIVISION multiple access (CDMA) is a multiplexing technique where a number of users simultaneously access a transmission channel by modulating and spreading their signals with preassigned codewords. Multiplication of the signals modulates a carrier and spreads the spectrum [1]. At the receiver, the original signal of a given user is detected by correlating the received signal with the corresponding codeword. This correlation despreads the spectrum. The other user signals are not despread because their codes do not match. However, they may contribute to the interference noise [1]. In general, the noise due to the interfering signals is reduced by the ratio of the spreading bandwidth and the signal bandwidth. This ratio is known as the processing gain G_p.

The system capacity, i.e., the total sum of the bit rates of the users, of a synchronized CDMA (S-CDMA) system can be much higher than that of an asynchronous CDMA (A-CDMA) system [2]. The reason is that the capacity of an S-CDMA system is limited by the maximum number of different codewords, whereas that of an A-CDMA is limited by the interference noise. For a given set of N_u codewords with length N, the maximum normalized cross correlation between two codewords $\Phi_{\max}$ is lower bounded by the Welch bound [3]

$$\Phi_{\max}^2 \geq \frac{\frac{N_u}{N} - 1}{N_u - 1}. \tag{1}$$

Two well-known sets of codewords satisfy the Welch bound with equality, namely, Gold codes for which $N_u = N + 1$ so that $\Phi_{\max} = 1/N$ and Walsh–Hadamard codes for which $N_u = N$ so that $\Phi_{\max} = 0$ [4]. Walsh–Hadamard codes have these ideal cross-correlation properties, because all the codewords are mutually orthogonal. This implies that in an S-CDMA system using Walsh–Hadamard codes the interference noise is zero. A-CDMA is a promising technology for mobile communications, where the transmission delay between the users and the receiver fluctuates in time. The reason is that the magnitude of the interference noise is relatively insensitive to the timing between the users. Only the timing accuracy between the spreading by the user and the despreading by the receiver is of importance. In contrast, S-CDMA requires accurate synchronization between all transmitters. If one of the users is not properly synchronized, it causes interference noise in the received signal for all other users. In the particular case of the digital video broadcasting return channel (DVB-RC) system for community antenna television (CATV), it is possible to synchronize, via ranging techniques, the users with an accuracy which is determined by the clock of the receiving head-end station. This clock also determines the timing accuracy of the despreading code for the particular user. Thus, the timing between the users has the same accuracy as the timing of the spreading code and despreading code of a particular user. As there always remains a nonperfect synchronization, such a system is denoted as quasi-synchronous CDMA (QS-CDMA).

This paper studies the performance of QS-CDMA systems with Walsh–Hadamard codewords and with high-order modulation schemes: M-level quadrature amplitude modulation (M-QAM) and M-level phase-shift keying (M-PSK) are compared with respect to the bit-error rate (BER). To this end, we adopt two approaches. Firstly, we calculate the maximum synchronization error that can be tolerated so that complete error-free despreading is guaranteed. Secondly, we calculate the BER under the assumption that the interference noise adds like white Gaussian noise to the user signal. In this

Paper approved by E. S. Sousa, the Editor for CDMA Systems of the IEEE Communications Society. Manuscript received April 7, 1999; revised April 17, 2000.

The author is with the Philips Semiconductors Systems Laboratory, Eindhoven (PS-SLE), 5600 MD Eindhoven, The Netherlands (e-mail: wim.van.houtum@philips.com).

Publisher Item Identifier S 0090-6778(01)05764-6.

second approach, thermal noise is included as well. The first approach provides insight in the synchronization demands for QS-CDMA systems. The second approach yields the expected system performance under operational conditions.

The outline is as follows. Section II describes the QS-CDMA system with binary phase-shift keying (BPSK). Section III analyzes the QS-CDMA system with M-QAM and M-PSK resulting in closed expressions for the BERs. Section IV shows BER versus signal-to-noise ratio (SNR) curves based on the expressions obtained in Section III.

All the closed expressions are obtained with a rectangular shape of the chip-pulse due to the unlimited possibilities of chip-pulse shapes. We would like to address to the interested reader, with the help of this paper, to calculate the closed expressions for their particular chip-pulse shapes. Also, the Walsh–Hadamard codewords are in this paper directly applied on the data symbols, they are not randomized, because the assumption is made that the data symbols are identically and independently distributed (i.i.d.).

II. QS-CDMA WITH BPSK

This section introduces CDMA with Walsh–Hadamard codewords, analyzes the correlation properties of these codewords as well as the performance of QS-CDMA with the simplest modulation technique, BPSK.

A. CDMA with Synchronization Errors

We consider a system with N_u different users that simultaneously share a transmission channel through CDMA. A user n $(n = 0, 1, \ldots, N_u - 1)$ transmits data symbols $a_i^n = -1$ or 1 after multiplication with the preassigned Walsh–Hadamard codewords $C_n(t)$. The transmitted signal $b_n(t)$ can thus be written as

$$b_n(t) = A_n \sum_{i=-\infty}^{\infty} a_i^n C_n(t - iT_s), \qquad n = 0, \ldots, N_u - 1 \tag{2}$$

with amplitude A_n and symbol duration T_s. The Walsh–Hadamard codeword is given by

$$C_n(t) = \sum_{j=0}^{N-1} c_j^n h(t - jT_c) \tag{3}$$

with $T_s = NT_c$ and $c_j^n = -1$ or $+1$ the elements of the nth Walsh–Hadamard codeword with chip duration T_c, and these Walsh–Hadamard Codewords can be constructed by taking the rows of the matrix H_N, shown as follows:

$$H_N = \begin{bmatrix} H_{N-1} & H_{N-1} \\ H_{N-1} & -H_{N-1} \end{bmatrix} \qquad H_0 = [1]. \tag{4}$$

The function $h(t) = 1$ if $0 < t < T_c$, and $h(t) = 0$ otherwise.

The received signal $r(t)$ is the summation of all the N_u signals

$$r(t) = \sum_{n=0}^{N_u-1} b_n(t - \tau_n) \tag{5}$$

where $\tau_n \in [-T_c, T_c]$ is the time shift between the transmitted and received signal of user n. To obtain, via a correlation-receiver [8], the desired signal $\tilde{a}_k^u$, the signal $r(t)$ has to be multiplied with the Walsh–Hadamard code $C_u(t)$ and integrated over the symbol duration

$$\begin{aligned} \tilde{a}_k^u &= \frac{1}{T_s} \int_0^{T_s} C_u(t) r(t + kT_s) dt \\ &= \frac{1}{T_s} \int_0^{T_s} C_u(t) \\ &\quad \times \left[\sum_{n=0}^{N_u-1} A_n \sum_{i=-\infty}^{\infty} a_i^n C_n(t + (k - i)T_s - \tau_n) \right] dt. \end{aligned} \tag{6}$$

Due to the time shift τ_u between the spreading and despreading code of user u, the integration not only contains the cross correlation from a_k^n but also from $a_{k\pm1}^n$. This minor contribution can be neglected when $\tau_u < T_c$ [5]. This yields for the received symbol

$$\begin{aligned} \tilde{a}_k^u &= \frac{1}{T_s} \int_0^{T_s} C_u(t) \left[\sum_{n=0}^{N_u-1} A_n a_k^n C_n(t - \tau_n) \right] dt \\ &= A_u a_k^u \phi_{uu}(\tau_u) + \sum_{n=0, n\neq u}^{N_u-1} A_n a_k^n \phi_{un}(\tau_n) \end{aligned} \tag{7}$$

where

$$\phi_{un}(\tau_n) \doteq \frac{1}{NT_c} \int_0^{NT_c} C_u(t) C_n(t - \tau_n) dt \tag{8}$$

is the correlation function between Walsh–Hadamard codeword $C_u(t)$ and Walsh–Hadamard codeword $C_n(t)$ shifted over τ_n. Equation (7) shows that the autocorrelation function $\phi_{uu}(\tau_u)$ is related to the wanted data stream a_i^u and the cross-correlation functions $\phi_{un}(\tau_n)$ to the $N_u - 1$ interfering data streams. Note that in the case of perfect synchronization $\tau_n = 0$, we have $\phi_{un}(0) = \delta_{un}$. The correlation values for $\tau_n = T_c$ can be expressed in the correlation matrix. Equation (9) shows the correlation matrix for a Walsh–Hadamard codeword set with length $N = 8$.

$$\phi_{kn}(T_c) = \begin{bmatrix} 1 & 0 & 0 & 0 & 0 & 0 & 0 & 0 \\ 0 & -1 & 0 & 0 & 0 & 0 & 0 & 0 \\ 0 & 0 & 0 & -1 & 0 & 0 & 0 & 0 \\ 0 & 0 & 1 & 0 & 0 & 0 & 0 & 0 \\ 0 & 0 & 0 & 0 & \frac{1}{2} & \frac{-1}{2} & \frac{-1}{2} & \frac{-1}{2} \\ 0 & 0 & 0 & 0 & \frac{1}{2} & \frac{-1}{2} & \frac{1}{2} & \frac{1}{2} \\ 0 & 0 & 0 & 0 & \frac{1}{2} & \frac{1}{2} & \frac{1}{2} & \frac{-1}{2} \\ 0 & 0 & 0 & 0 & \frac{-1}{2} & \frac{-1}{2} & \frac{1}{2} & \frac{-1}{2} \end{bmatrix} \tag{9}$$

B. Walsh–Hadamard Code Properties

From (7), it follows that the original user data symbol a_k^u can be deduced from the received signal as long as

$$A_u \phi_{uu}(\tau_u) + \sum_{n=0, n\neq u}^{N_u-1} A_n \left(\frac{a_k^n}{a_k^u} \right) \phi_{un}(\tau_n) > 0. \tag{10}$$

From now on, we will assume that the amplitudes of all users are equal, i.e., $A_n = A_p$ for all n, p. We see from (10) that error-free reception of a_k^u depends on the values of the other user bits a_k^n. The occurrence of error-free reception may therefore be regarded as a statistical process. We will follow two ways to study the influence of synchronization errors. Firstly, we study the worst-case situation under which (10) is guaranteed to be fulfilled so that the reception is completely error-free. This strict condition corresponds to a maximum allowable synchronization error. This analysis is valuable from a conceptual perspective but does not include other noise than the interference noise. In the second approach, both the interference noise and the thermal noise are treated on the same footing. By assuming that these noise sources can be modeled as Gaussian white noise, we calculate the BER as a function of the SNR.

For the strict-condition analysis, (10) is transformed into

$$\phi_{uu}(\tau_u) - \sum_{n=0,n\neq u}^{N_u-1} |\phi_{un}(\tau_n)| > 0. \tag{11}$$

Let us now have a closer look at the two terms at the left-hand side of (11).

Due to the rectangular shape of $h(t)$, the autocorrelation function $\phi_{uu}(\tau_u)$ is a linear decreasing function of τ_u which is symmetrical round $\tau_u = 0$ with $\tau_u \in [-T_c, T_c]$. To determine this function, we only need two points. The value $\phi_{uu}(0) = 1$ is the first point and the value $\phi_{uu}(T_c)$ is the second. The value $\phi_{uu}(T_c)$ varies between 1 (codeword 0) and -1 (codeword 1) as can be seen from (9). The slope of the autocorrelation function therefore depends on the codeword of the code set. The autocorrelation function can be written as

$$\phi_{uu}(\tau_u) = \frac{\phi_{uu}(T_c) - 1}{T_c}\tau_u + 1, \qquad 0 \le \tau_u \le T_c \tag{12}$$

for symmetry reasons of $\phi_{uu}(\tau_u)$, only $\tau_u \in [0, T_c]$ is considered. Due to the rectangular shape of the Walsh–Hadamard code bits, we find for the cross-correlation function

$$\phi_{un}(\tau_n) = \frac{\tau_n}{T_c}\phi_{un}(T_c), \qquad 0 \le \tau_n \le T_c \tag{13}$$

for symmetry reasons of $|\phi_{un}(\tau_n)|$, only $\tau_n \in [0, T_c]$ is considered. This is a linear increasing function starting at zero.

Substitution of (12) and (13) into (11) yields

$$\frac{\phi_{uu}(T_c) - 1}{T_c}\tau_u + 1 - \frac{\sum_{n=0,n\neq u}^{N_u-1} \tau_n |\phi_{un}(T_c)|}{T_c} > 0, \quad 0 \le \tau_u, \tau_n \le T_c. \tag{14}$$

It follows from (14) that whenever the autocorrelation value is larger than the cross-correlation value, it is possible to recover the desired data stream a_k^u. If the autocorrelation value equals the cross-correlation value, due to a certain time shift, then there is no possibility to recover the desired data without errors.

The strict condition that no errors occur requires that all synchronization errors τ_n are smaller than the maximum synchronization error ΔT. Which is the maximum synchronization error in the worst-case scenario, the strict condition that no errors are allowed. From (14), it follows that

$$\frac{\phi_{uu}(T_c) - 1}{T_c}\Delta T + 1 = \frac{\sum_{n=0,n\neq u}^{N_u-1} |\phi_{un}(T_c)|}{T_c}\Delta T \tag{15}$$

which can be rewritten as

$$\Delta T = \frac{1}{\sum_{n=0,n\neq u}^{N_u-1} |\phi_{un}(T_c)| - \phi_{uu}(T_c) + 1} T_c \tag{16}$$

with ΔT is upper bounded by T_c.

In the case that $\sum_{n=0,n\neq u}^{N_u-1} |\phi_{un}(T_c)| - \phi_{uu}(T_c) + 1 = 0$, ΔT tends to infinity, so that we have an ideal codeword which never introduces any errors due to a time shift. Only the first codeword of the Walsh–Hadamard code set has this property. This particular case will be excluded for further calculations.

The maximum value of ΔT which equals T_c is obtained if $\sum_{n=0,n\neq u}^{N_u-1} |\phi_{un}(T_c)| \le \phi_{uu}(T_c)$. This means that the Walsh–Hadamard codewords introduce no errors within T_c (the best case). For a set of N Walsh–Hadamard codewords, the maximum synchronization error is the minimum of (16) over all codewords u. This yields

$$\Delta T = \frac{1}{\max_u \left\{\sum_{n=0,n\neq u}^{N_u-1} |\phi_{un}(T_c)| - \phi_{uu}(T_c)\right\} + 1} T_c. \tag{17}$$

We note that in practice the magnitude of ΔT is dictated by the chosen hardware and by the transmission environment. The strict-condition analysis provides a means to estimate and to dimension the system capacity for the dictated ΔT.

C. Strict System Capacity of QS-CDMA with BPSK

BPSK is an elementary modulation method that maps binary symbols (-1 or 1) into a single waveform with two corresponding discrete phases. The amplitude of this waveform is constant and its period is equal to the chip duration T_c.

If a CDMA system with Walsh–Hadamard codewords utilizes BPSK, the system capacity (the total bit rate which can be detected) $C_{\max}$ of the N_u users for a given maximum synchronization error ΔT follows from (17):

$$\begin{aligned} C_{\max} &= \frac{1}{T_c} \\ &= \frac{\frac{1}{\Delta T}}{\max_u \left\{\sum_{n=0,n\neq u}^{N_u-1} |\phi_{un}(T_c)| - \phi_{uu}(T_c)\right\} + 1}. \end{aligned} \tag{18}$$

The maximum bit rate for each user is given by

$$R_{b_{\max}} = \frac{C_{\max}}{N}. \tag{19}$$

The bit rate $R_{b_{\max}}$ and the capacity $C_{\max}$ are shown for different values of N in Figs. 1 and 2, respectively. As the interference noise increases with N, the capacity $C_{\max}$ decreases with N. Note that these results are subject to a maximum synchronization error ΔT. Inversely, one can utilize (18) to determine

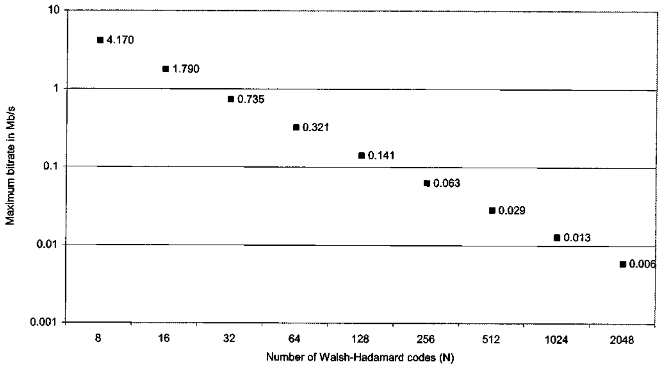

Fig. 1. The maximum bit rate $R_{b_{\max}}$ of a QS-CDMA system with BPSK for a maximum synchronization error $\Delta T = 10$ ns as a function of the number of Walsh–Hadamard codes N, where the number of users $N_u = N$.

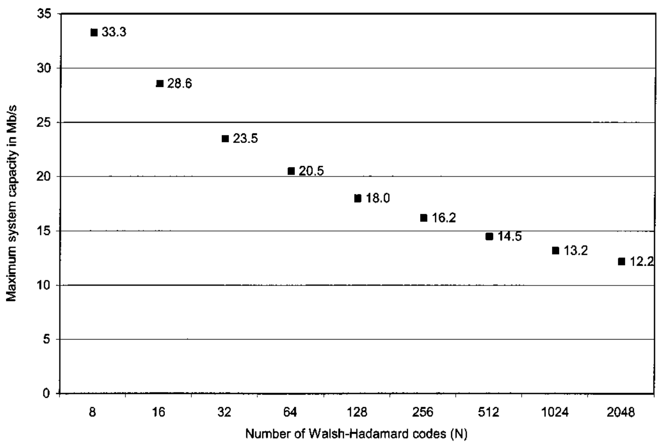

Fig. 2. The maximum system capacity $C_{\max}$ of a QS-CDMA system with BPSK for a maximum synchronization error $\Delta T = 10$ ns as a function of the number of Walsh–Hadamard codes N, where the number of users $N_u = N$.

TABLE I

MAXIMUM NUMBER OF WALSH–HADAMARD CODEWORDS N THAT CAN BE SUSTAINED IN A QS-CDMA SYSTEM WITH ERROR-FREE RECEPTION FOR A GIVEN BANDWIDTH OF 10 MHz ($T_c = 100$ ns) AND A GIVEN MAXIMUM SYNCHRONIZATION ERROR $\Delta T = 10$ ns. MAXIMUM SYSTEM CAPACITY $C_{\max} = m/T_c$ IS GIVEN AS WELL

Modulation method	N	C_{max} (Mb/s)
BPSK	8192	10
QPSK	1024	20
8-PSK	64	30
16-PSK	8	40
64-PSK	1	60
16-QAM	16	40
64-QAM	4	60
256-QAM	1	80

the maximum number of users $N = N_u$ for a given value of the bandwidth $(1/T_c)$ and a given ΔT, see Table I.

III. ANALYSIS OF QS-CDMA WITH HIGH-ORDER MODULATION

Spectral efficiency is the transmission efficiency of a digital modulation method measured in units of bits/second/Hertz. A higher-order modulation method can be used to transmit the coded data streams with higher spectral efficiency than BPSK. The modulation process involves switching or keying the amplitude, frequency, and/or phase of the carrier according to the data symbols. In most high-order digital modulation schemes, the in-phase carrier (I) and a $\pi/2$-shifted carrier, the quadrature carrier (Q), are used. For M-ary digital modulation, where $M \doteq 2^m$ is the number of symbols consisting of m bits, the symbol duration $T_s = mT_b$ where T_b is the bit duration.

If the symbols are modulated by keying phases and amplitudes, then we have M-QAM. If only the phases of the symbols are keyed, then we have M-PSK).

A symbol is the addition of the in-phase and quadrature carrier. These symbols can be expressed as points in a complex plane where the x-axis and y-axis represent the in-phase carrier and quadrature carrier, respectively. Such a representation is called a constellation diagram. Fig. 3 shows the constellation diagrams of 16-PSK and of 64-QAM.

In M-QAM, the symbols a_k^n of user n can be represented in the constellation diagram as points

$$a = (i, j), \qquad i, j = -\sqrt{M}+1, -\sqrt{M}+3, \ldots, \sqrt{M}-1 \tag{20}$$

where $i \times A_n$ and $j \times A_n$ representing the amplitude values of the in-phase carrier and the quadrature carrier, respectively, for the M-QAM symbols a_k^n of user n.

The average signal energy of user n, E_s^n, is given by

$$\begin{aligned} E_s^n &= \frac{1}{M}\sum_{i,j} E(a) = \frac{1}{M}A_n^2 \sum_{i,j}\left(i^2 + j^2\right) \\ &= \frac{4}{\sqrt{M}}A_n^2 \sum_{i=1}^{(1/2)\sqrt{M}} (2i-1)^2 = \frac{2}{3}(M-1)A_n^2. \end{aligned} \tag{21}$$

In M-PSK, the symbols a_k^n can be written as

$$a = \left(\cos\left(i\frac{2\pi}{M}\right), \sin\left(i\frac{2\pi}{M}\right)\right), \qquad i = \{0, 1, \ldots, M-1\}. \tag{22}$$

Here, the average signal energy is simply $E_s^n = A_n^2$.

The analysis of the influence of synchronization errors in a QS-CDMA system with either M-QAM or M-PSK proceeds analogously to the analysis for BPSK in the previous section, with the modification that the binary valued symbols a_k^n are now symbols in the complex plane. Note that the orientations of the constellation diagrams of different users are uncorrelated.

In Section III-A and Section III-B, we analyze the strict condition system capacity of a QS-CDMA system with M-QAM and M-PSK, respectively. Sections III-C and III-D study the BER as a function of the SNR. In Section III-E, the results of Sections III-C and III-D are averaged for the case that the synchronization errors are uniformly distributed within a given interval.

A. Strict Condition Analysis of M-QAM

The reception of an M-QAM symbol $\tilde{a}_k^u$ is error-free when it can be unambiguously reduced to the original symbol a_k^u. This implies that the received symbol must be placed at the right point in the constellation diagram. For M-QAM, we need to make the distinction between the following three types of symbols (see Fig. 3). 1) **Inner points** that represent the M-QAM symbols

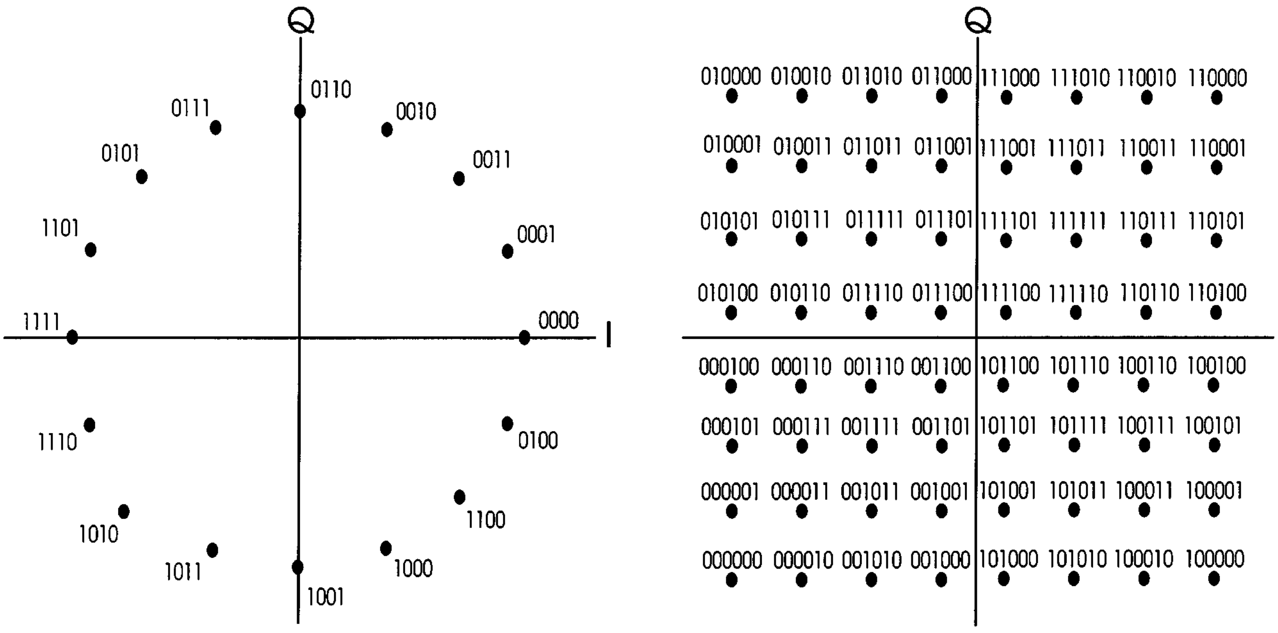

(a) (b)

Fig. 3. Constellation diagrams of (a) 16-PSK and (b) 64-QAM.

at the inner side of the square constellation diagram. 2) **Outer points** that represent the M-QAM symbols at the outer side of the square constellation diagram. 3) **Corner points** that represent the M-QAM symbols at the corners of the square constellation diagram. For error-free reception of inner points, one has the condition for the real ($\Re$) and ($\Im$) imaginary parts

$$|\Re(\tilde{a}_k^u - d_u a_k^u)| < d_u, \tag{23}$$

$$|\Im(\tilde{a}_k^u - d_u a_k^u)| < d_u \tag{24}$$

where d_u is the "grid size" of the M-QAM constellation at the receiver [9]. Assuming that the receiver adjusts to the magnitude of the received signal for user u, one has

$$d_u a_k^u = \tilde{a}_k^u \longrightarrow d_u = \phi_{uu}(\tau_u) A_u. \tag{25}$$

For outer and corner points the conditions (23) and (24) are slightly modified. For example, for a symbol at the top row of the constellation diagram, we must replace (24) by [9]

$$\Im(\tilde{a}_k^u - d_u a_k^u) > -d_u. \tag{26}$$

Similar conditions apply to the bottom row, as well as the outer left and outer right column [9]. Substitution of (7) into (23) and taking into account that the constellation diagrams are randomly oriented yields

$$\left| \Re\left(\sum_{n \neq u} A_n \phi_{un}(\tau_n) e^{i\theta_n} a_k^n \right) \right| < d_u \tag{27}$$

where $\theta_n \in [0, 2\pi]$ denotes the relative orientation of the constellation diagram of user n with respect to user u. Similar results can be obtained for (24) and (7). Just as in the previous section, we assume from now on that the amplitudes A_n are equal for all n. To ensure that all symbols are correctly received, we must consider the worst-case situation where the interference noise caused by the other users is maximal. Clearly, this is the case when the interfering symbols a_k^n are at corner points and when the constellation diagram is rotated over 45°, i.e., $\theta_n = \pm\pi/4, \pm 3\pi/4$. As a result, (23)–(27) leads to the condition

$$\sqrt{2}\left(\sqrt{M} - 1\right) \sum_{n \neq u} |\phi_{un}(\tau_n)| < \phi_{uu}(\tau_u) \tag{28}$$

so that using (12) and (13), we have

$$\sqrt{2}\left(\sqrt{M} - 1\right) \sum_{n \neq u} \frac{\tau_n}{T_c} |\phi_{un}(T_c)| < 1 - \frac{\tau_u}{T_c} + \frac{\tau_u}{T_c} \phi_{uu}(T_c). \tag{29}$$

The strict condition that no errors occur requires that all synchronization errors τ_n are smaller than the maximum synchronization error ΔT, given by

$$\Delta T = \frac{T_c}{\sqrt{2}\left(\sqrt{M} - 1\right) \sum_{n=0, n \neq u}^{N_u - 1} |\phi_{un}(T_c)| - \phi_{uu}(T_c) + 1}. \tag{30}$$

Equation (30) allows us to determine the maximum capacity of a QS-CDMA system with M-QAM and a maximum synchronization error ΔT subject to the condition of error-free reception

$$\begin{aligned} C_{\max}^{\mathrm{QAM}} &= \frac{m}{T_c} \\ &= \frac{\frac{m}{\Delta T}}{\sqrt{2}\left(\sqrt{M} - 1\right) \sum_{n=0, n \neq u}^{N_u - 1} |\phi_{un}(T_c)| - \phi_{uu}(T_c) + 1}. \end{aligned} \tag{31}$$

From (31), the maximum bit rate of one data stream can be calculated as

$$R_{b_{\max}}^{\mathrm{QAM}} = \frac{C_{\max}^{\mathrm{QAM}}}{N}. \tag{32}$$

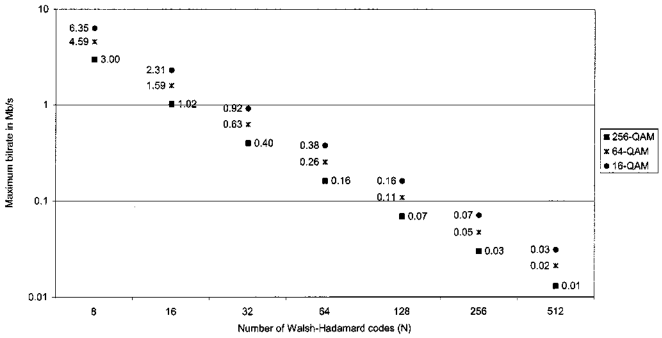

Fig. 4. The maximum bit rate $R^{\mathrm{QAM}}_{b_{\max}}$ for a maximum synchronization error of $\Delta T = 10$ ns as a function of the number of Walsh–Hadamard codewords N.

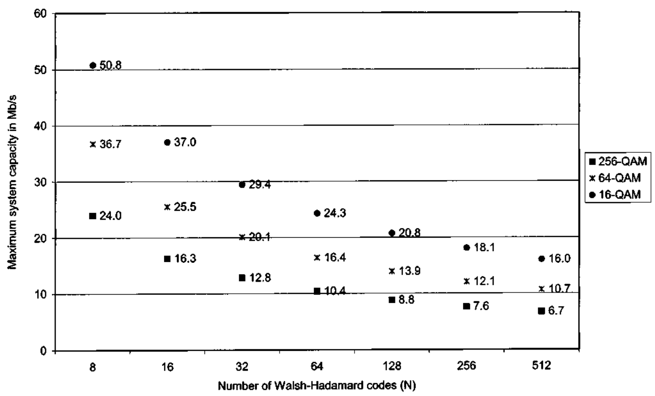

Fig. 5. The maximum system capacity $C^{\mathrm{QAM}}_{\max}$ for a maximum synchronization error of $\Delta T = 10$ ns as a function of the number of Walsh–Hadamard codewords N.

The quantities $R^{\mathrm{QAM}}_{b_{\max}}$ and $C^{\mathrm{QAM}}_{\max}$ for 16-QAM, 64-QAM, and 256-QAM are shown in Figs. 4 and 5, respectively.

We have found that ΔT and thus the multiuser interference depends on the modulation order m. Larger m leads to an increased ratio between the maximum amplitude and the distance between two neighboring symbols. Therefore, the larger m, the more sensitive the system is for interference noise.

Complementary to the results shown in Figs. 4 and 5, one can utilize (31) to determine the maximum value of N for given values of ΔT and T_c (see Table I).

B. Strict Condition Analysis of M-PSK

Error-free reception of an M-PSK symbol a^u_k occurs when the despreaded symbol $\tilde{a}^u_k$ can be distributed in the right circle segment in the M-PSK constellation diagram (see Fig. 3). This implies

$$|\arg(\tilde{a}^u_k) - \arg(a^u_k)| < \frac{\pi}{M} \tag{33}$$

where $\arg(z)$ denotes the phase of the complex number z. Again, we assume that the amplitudes A_n are equal for all n. Without loss of generality, we may state $a^u_k = (1, 0)$, so that $\arg(a^u_k) = 0$. Substitution of (12) and (13) now yields

$$\left|\arg\left[\phi_{uu}(\tau_u) + \sum_{n\neq u} \phi_{un}(\tau_n) e^{i\theta_n} a^n_k\right]\right| < \frac{\pi}{M} \tag{34}$$

where $\theta_n \in [0, 2\pi]$ denotes the relative orientation of user n with respect to user u. For the strict-condition analysis, we seek the symbols a^n_k that results in the maximal interference noise. From the M-PSK constellation diagram, it can be shown that the interference contribution is maximally disturbing when

$$\arg\left(a^n_k e^{i\theta_n}\right) = \pm\left(\frac{\pi}{2} + \frac{2\pi}{M}\right). \tag{35}$$

Using trigonometric analysis (34) and (35) can be rewritten as

$$\sum_{n\neq u} |\phi_{un}(\tau_n)| < \sin\left(\frac{\pi}{M}\right) \phi_{uu}(\tau_u). \tag{36}$$

From this point, the analysis is identical to the M-QAM case in Section III-A. The resulting maximum synchronization error for error-free reception is given by

$$\Delta T = \frac{T_c}{\sin^{-1}\left(\frac{\pi}{M}\right) \sum_{n=0,n\neq u}^{N_u-1} |\phi_{un}(T_c)| - \phi_{uu}(T_c) + 1}. \tag{37}$$

Before presenting the results for the system capacity, we briefly compare (37) with the maximum synchronization error for M-QAM as given in (30). For $M = 4$, the results are identical, as expected. Noting that $\sin^{-1} \pi/M \to M/\pi$ as M increases, we observe that the timing requirements of M-QAM are much more favorable than that of M-PSK. The reason is that the distance between neighboring symbols decreases much faster for M-PSK than for M-QAM as M increases (see Fig. 3).

The system capacity subject to the condition of error-free reception is given by

$$\begin{aligned} C^{\mathrm{PSK}}_{\max} &= \frac{m}{T_c} \\ &= \frac{m}{\left(\sin^{-1}\left(\frac{\pi}{M}\right) \sum_{n=0,n\neq u}^{N_u-1} |\phi_{un}(T_c)| - \phi_{uu}(T_c) + 1\right)\Delta T}. \end{aligned} \tag{38}$$

From (38), the maximum bit rate of one data stream a^u_i with M-PSK modulation can be calculated for a given ΔT

$$R^{\mathrm{PSK}}_{b_{\max}} = \frac{C^{\mathrm{PSK}}_{\max}}{N}. \tag{39}$$

The quantities $R^{\mathrm{PSK}}_{b_{\max}}$ and $C^{\mathrm{PSK}}_{\max}$ for QPSK, 8-PSK, and 16-PSK are shown in Figs. 6 and 7, respectively.

Furthermore, we have utilized (38) to calculate the maximum number of Walsh–Hadamard codewords N that can be supported in a QS-CDMA system with M-PSK with a maximum synchronization error $\Delta T = 10$ ns and a chip-time $T_c = 100$ ns (see Table I).

This table lists the maximum number of Walsh–Hadamard codewords (and thus the maximum number of users) N that can be supported in a QS-CDMA system with a given bandwidth ($T_c = 100$ ns) and a given maximum synchronization error $\Delta T = 10$ ns for a range of modulation methods. For this maximum number of users, the interference noise is still so small that all symbols from all users can be received without any errors. If the modulation order increases, the QS-CDMA system

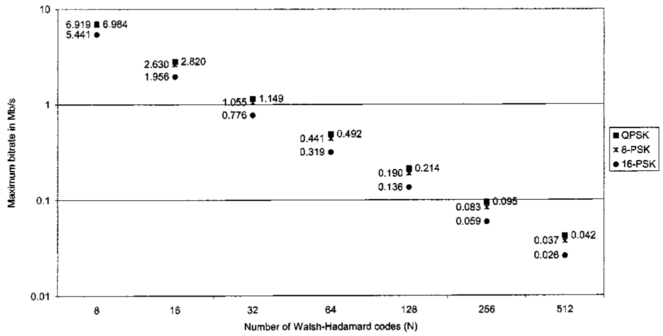

Fig. 6. The maximum bit rate $R_{b_{\max}}^{\mathrm{PSK}}$ for a maximum synchronization error of $\Delta T = 10$ ns as a function of the number of Walsh–Hadamard codewords N.

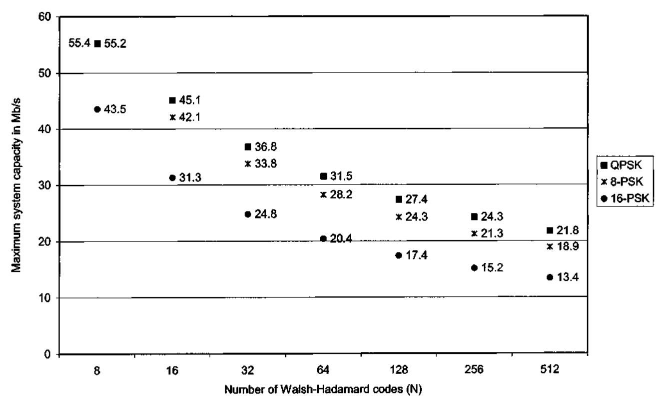

Fig. 7. The maximum system capacity $C_{\max}^{\mathrm{PSK}}$ for a maximum synchronization error of $\Delta T = 10$ ns as a function of the number of Walsh–Hadamard codewords N.

becomes more sensitive to synchronization errors, so that for the given constraints the maximum number of users decreases. For 256-QAM and 64-PSK, CDMA is no longer possible and $N = 1$.

C. BER of QS-CDMA with M-QAM

In this section, the BER as a function of the SNR for M-QAM $(M = 16, 64, \ldots)$ is considered. This BER will be determined by three types of distortion. Firstly, there is the decreasing of the symbol amplitude due to imperfect synchronization between receiver and transmitter. Secondly, interference noise is generated because the other users are not synchronized. The third distortion is the thermal noise. The assumption is made that the amplitude of this thermal noise has a Gaussian (normal) distribution with zero mean and variance $(N_o/2)$, no correlation (flat spectrum), and is added to the signal. This is called additive white Gaussian Noise (AWGN), where the amplitude is distributed according to the probability density function [9]

$$p_n(\alpha) \doteq \frac{1}{\sqrt{\pi N_o}} e^{(-\alpha^2/N_o)}. \tag{40}$$

If the amplitude distortion of the in-phase carrier and the quadrature carrier of the M-QAM symbols lies between $-d_u$ and d_u, the receiver detects the transmitted M-QAM symbols without errors [8]. The probability that the thermal noise lies between these levels for every M-QAM symbol can be calculated by

$$P[-d_u < n < d_u] = \int_{-d_u}^{d_u} p_n(\alpha) d\alpha. \tag{41}$$

Every M-QAM symbol is represented by a point at the M-QAM square constellation diagram. The probability of correct detection of the transmitted M-QAM symbols can be calculated with (41). The probability calculation has to be carried out for every point of the constellation diagram. From a straightforward calculation it follows that the probability of detecting the transmitted M-QAM symbol correctly is given by:

$$\begin{aligned} P[C] = &\frac{1}{M}\left[\left(\sqrt{M}-2\right)^2(1-2p)^2 \right. \\ &\left. + 4\left(\sqrt{M}-2\right)(1-2p)(1-p) + 4(1-p)^2\right] \\ = &1 - 4\left(1-\frac{1}{\sqrt{M}}\right) Q\left(\sqrt{\frac{2d_u^2}{N_o}}\right) \\ &+ 4\left(1-\frac{1}{\sqrt{M}}\right)^2 \left[Q\left(\sqrt{\frac{2d_u^2}{N_o}}\right)\right]^2 \end{aligned} \tag{42}$$

where

$$p \doteq \int_{d_u}^{\infty} p_n(\alpha) d\alpha = Q\left(\sqrt{\frac{2d_u^2}{N_o}}\right). \tag{43}$$

The probability of detecting a wrong M-QAM symbol, the symbol-error rate (SER), is given by

$$\begin{aligned} \mathrm{SER} = &1 - P[C] \\ = &4\left(1-\frac{1}{\sqrt{M}}\right) Q\left(\sqrt{\frac{2d_u^2}{N_o}}\right) \\ &\times \left[1 - \left(1-\frac{1}{\sqrt{M}}\right) Q\left(\sqrt{\frac{2d_u^2}{N_o}}\right)\right]. \end{aligned} \tag{44}$$

Substitution of (21) and (25) into (44) yields

$$\begin{aligned} \mathrm{SER} = &4\left(1-\frac{1}{\sqrt{M}}\right) Q\left(\sqrt{\frac{\frac{3\phi_{uu}^2(\tau_u)}{(M-1)} \cdot E_s^u}{N_o}}\right) \\ &\times \left[1 - \left(1-\frac{1}{\sqrt{M}}\right) Q\left(\sqrt{\frac{\frac{3\phi_{uu}^2(\tau_u)}{(M-1)} \cdot E_s^u}{N_o}}\right)\right] \end{aligned} \tag{45}$$

the SER of user u. The SER as computed in (45) takes only the following two distortions into account, namely: 1) thermal noise and 2) imperfect synchronization between transmitter and receiver of user u. The third distortion is caused by the other users because the cross-correlation values of the used Walsh–Hadamard-codes are not zero in case of imperfect synchronization. This leads to multiple-access interference or self noise. Since the symbols a_i^n are i.i.d., we may threat this self noise as Gaussian noise

$$N_{\text{interference}}^n = \frac{2}{3}(M-1)A_n^2\phi_{un}^2(\tau_n) = \phi_{un}^2(\tau_n)E_s^n. \quad (46)$$

Substitution into (45) yields

$$\begin{aligned}\text{SER} =& 4\left(1-\frac{1}{\sqrt{M}}\right) \\ &\times Q\left(\sqrt{\frac{\frac{3\phi_{uu}^2(\tau_u)}{(M-1)}\cdot E_s^u}{N_o+\sum_{n=0,n\neq u}^{N_u-1}\phi_{un}^2(\tau_n)E_s^n}}\right) \\ &\times\left[1-\left(1-\frac{1}{\sqrt{M}}\right)\right. \\ &\left.\times Q\left(\sqrt{\frac{\frac{3\phi_{uu}^2(\tau_u)}{(M-1)}\cdot E_s^u}{N_o+\sum_{n=0,n\neq u}^{N_u-1}\phi_{un}^2(\tau_n)E_s^n}}\right)\right] \quad (47)\end{aligned}$$

which can be approximated by

$$\begin{aligned}\text{SER} \approx& 4\left(1-\frac{1}{\sqrt{M}}\right) \\ &\times Q\left(\sqrt{\frac{\frac{3\phi_{uu}^2(\tau_u)}{(M-1)}\cdot E_s^u}{N_o+\sum_{n=0,n\neq u}^{N_u-1}\phi_{un}^2(\tau_n)E_s^n}}\right). \quad (48)\end{aligned}$$

To obtain the BER as function of the SNR, the relation between the BER and the SER has to be found. This relation depends on how the bits are mapped on the 2^m-QAM symbols. If the SNR is large enough, the SER is dominated by symbol errors between nearest neighbors [11] and due to Gray mapping every symbol error causes one bit error [9]. The bit rate is m times the symbol rate, so the ratio between the SER and the BER is the modulation order m

$$\text{BER} = \frac{1}{m}\text{SER}. \quad (49)$$

Substitution of (49) into (47) yields

$$\begin{aligned}\text{BER} =& \frac{4}{m}\left(1-\frac{1}{\sqrt{M}}\right) \\ &\times Q\left(\sqrt{\frac{\frac{3\phi_{uu}^2(\tau_u)}{(M-1)}\cdot E_s^u}{N_o+\sum_{n=0,n\neq u}^{N_u-1}\phi_{un}^2(\tau_n)E_s^n}}\right) \\ &\times\left[1-\left(1-\frac{1}{\sqrt{M}}\right)\right. \\ &\left.\times Q\left(\sqrt{\frac{\frac{3\phi_{uu}^2(\tau_u)}{(M-1)}\cdot E_s^u}{N_o+\sum_{n=0,n\neq u}^{N_u-1}\phi_{un}^2(\tau_n)E_s^n}}\right)\right] \quad (50)\end{aligned}$$

which can be approximated by

$$\begin{aligned}\text{BER}_u^{\text{QAM}} \approx& \frac{4}{m}\left(1-\frac{1}{\sqrt{M}}\right) \\ &\times Q\left(\sqrt{\frac{\frac{3\phi_{uu}^2(\tau_u)}{(M-1)}\cdot E_s^u}{N_o+\sum_{n=0,n\neq u}^{N_u-1}\phi_{un}^2(\tau_n)E_s^n}}\right). \quad (51)\end{aligned}$$

D. BER of QS-CDMA with M-PSK

Every M-PSK symbol is represented by a point in a M-PSK circular constellation diagram, as shown in Fig. 3, where the horizontal axis represents the in-phase carrier and the vertical axis represents the quadrature carrier. In this section, the BER for M-PSK is considered.

The derivation done for M-PSK with QS-CDMA and Walsh–Hadamard codewords is similar to that for M-QAM. The final formula for M-PSK with the autocorrelation and cross-correlation functions can be composed of the results obtained for M-QAM and the theoretically well-known standard BER formula for M-PSK [9]

$$\text{BER} \approx \frac{2}{m}Q\left(\sqrt{\frac{2\sin^2\left(\frac{\pi}{M}\right)\cdot E_s}{N_o}}\right). \quad (52)$$

The Gaussian approximation for the self noise is also applicable in the M-PSK case [7]. If we look at (51), we see that the autocorrelation function $\phi_{uu}(\tau_u)$ is related to the signal energy E_s^u according to

$$\left(\frac{d_u}{\sin\left(\frac{\pi}{M}\right)}\right)^2 = \frac{A_u^2\phi_{uu}^2(\tau_u)}{\sin^2\left(\frac{\pi}{M}\right)} = \phi_{uu}^2(\tau_u)E_s^u. \quad (53)$$

Furthermore the cross-correlation function $\phi_{un}(\tau_n)$ determines the interference noise energy. With these results, we obtain for M-PSK

$$\text{BER}_u^{\text{PSK}} \approx \frac{2}{m}Q\left(\sqrt{\frac{2\sin^2\left(\frac{\pi}{M}\right)\cdot\phi_{uu}^2(\tau_u)\cdot E_s^u}{N_o+\sum_{n=0,n\neq u}^{N_u-1}\phi_{un}^2(\tau_n)E_s^n}}\right). \quad (54)$$

Remark: The calculation of the BER of user u with QPSK modulation $(m = 2, M = 4)$ in a full loaded $(N_u = N)$ QS-CDMA system with time shifts τ_u and $\{\tau_n\}$ gives with (54) the same result as with (51). This should be the case because 4-QAM and QPSK are equivalent [9].

E. BER for M-QAM and M-PSK for Uniformly Distributed Synchronization Errors

Equations (51) and (54) allow us to evaluate the BER for given values of τ_u and $\{\tau_n\}$. We now calculate the expected BER if the τ_u and $\{\tau_n\}$ are distributed uniformly between $-\Delta T$ and $+\Delta T$, where $0 < \Delta T \leq T_c/2$. This is a realistic distribution because in practical systems the synchronization errors of the users are independent from each other and can vary between zero and half the chip-time with equal probability. It is important to note that (51) and (54) are only valid if $\phi_{uu}(\tau_u) > 0$, this restricts the maximum value of τ_u to $T_c/2$. We utilize the expectation of the squared autocorrelation function

$$E\left(\phi_{uu}^2\right) \doteq \int_{-\Delta T}^{+\Delta T}\frac{1}{2\Delta T}\phi_{uu}^2(\tau_u)d\tau_u. \quad (55)$$

Using (12), we have

$$\begin{aligned}E\left(\phi_{uu}^2\right) =& \frac{\Delta T}{3T_c}\left[\frac{\Delta T}{T_c}\phi_{uu}(T_c)+3-\frac{\Delta T}{T_c}\right] \\ &\cdot\left[\phi_{uu}(T_c)-1\right]+1. \quad (56)\end{aligned}$$

Similarly, we find for the variance of the cross-correlation function

$$E\left(\phi_{un}^2\right) \doteq \int_{-\Delta T}^{+\Delta T} \frac{1}{2\Delta T}\phi_{un}^2(\tau_n)d\tau_n = \frac{1}{3}\left(\frac{\Delta T}{T_c}\right)^2 \phi_{un}^2(T_c). \tag{57}$$

Substitution of these results into (51) and (54) yields (58) and (59), shown at the bottom of the page, for the BER of user u with M-QAM and M-PSK, respectively.

Example: The calculation of the BER of user u with QPSK in a full loaded QS-CDMA system with $N_u = N = 8$ Walsh–Hadamard codewords and a time shift $\Delta T = T_c/3$.

We assign to user u codeword 7, this codeword has autocorrelation value $\phi_{77}(T_c) = -1/2$, and three nonzero cross-correlation components: $\phi_{74}(T_c) = -1/2$, $\phi_{75}(T_c) = 1/2$, and $\phi_{76}(T_c) = -1/2$.

Substitution into (58) yields

$$\mathrm{BER}^{(7)}\left(\frac{T_c}{3}\right) \approx Q\left(\sqrt{21\cdot\frac{\frac{E_s}{N_o}}{36+\frac{E_S}{N_o}}}\right).$$

In the limit case that $E_s/N_o \to \infty$ then

$$\lim_{(E_s/N_o)\to\infty} \mathrm{BER}^{(7)}\left(\frac{T_c}{3}\right) = Q\left(\sqrt{21}\right) \approx 2.3\times 10^{-6}$$

gives the BER-floor due to a synchronization error (time shift) of $\Delta T = T_c/3$[10]. The same result is obtained with (59).

IV. Results of QS-CDMA with Walsh-Hadamard Codewords and Higher-Order Modulation

In this section, the results of (58) and (59) are shown for QPSK, 16-PSK, and 16-QAM. The higher-order modulation methods 16-QAM and 16-PSK are compared with each other. We also make the comparison between the different codewords with 16-QAM at a constant timing error.

A. QS-CDMA with M-PSK and Different Timing Errors

This section describes the performances of QPSK used in a QS-CDMA system where the maximum number of users (length of codeword set) is $N = 8$. The BER of QS-CDMA with QPSK and 16-PSK for different timing errors are shown by Figs. 8 and 9, respectively.

Where ΔT is the practical system synchronization error between the codeword of the transmitter and receiver of the desired user and also between the transmitters of the other (undesired) users.

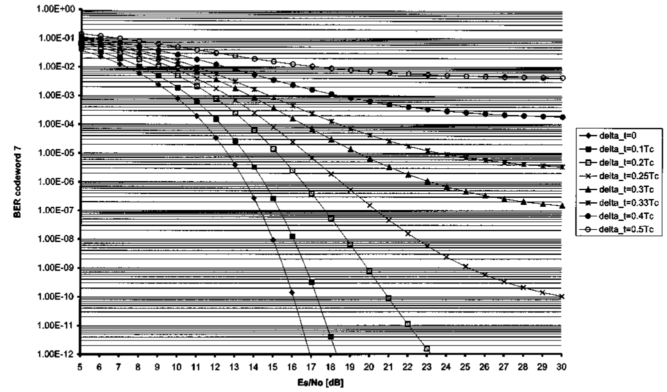

Fig. 8. BER in a QS-CDMA system with codeword 7 out of 8 Walsh–Hadamard codewords and QPSK for various timing errors ΔT.

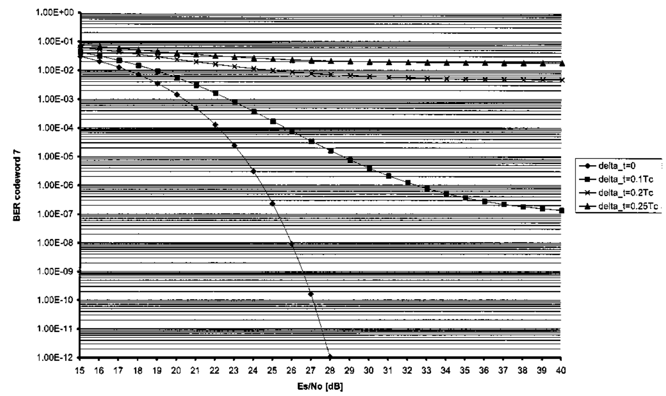

Fig. 9. BER in a QS-CDMA system with codeword 7 out of 8 Walsh–Hadamard codewords and 16-PSK for various timing errors ΔT.

Figs. 8 and 9 demonstrate that the timing error for 16-PSK has to be $\Delta T \leq 0.2T_c$ to obtain the same performance as with QPSK where $\Delta T = 0.5T_c$. This means that increasing the modulation index from two (QPSK) to four (16-PSK) and herewith creating the possibility to double the chip time T_c, with the same bit rate, we gain nothing. Because the allowed synchronization error for 16-PSK will be more than halved compared to QPSK.

B. QS-CDMA with 16-QAM and Different Timing Errors

This section describes the performances of 16-QAM used in a QS-CDMA system where the maximum number of users (length of codeword set) is $N = 8$. The BER of QS-CDMA with 16-QAM for different timing errors is shown in Fig. 10.

$$\mathrm{BER}_u^{\mathrm{QAM}}(\Delta T) \approx \frac{4}{m}\left(1-\frac{1}{\sqrt{M}}\right) Q\left(\sqrt{\frac{\frac{\Delta T\left(\frac{\Delta T}{T_c}\phi_{uu}(T_c)+3-\frac{\Delta T}{T_c}\right)(\phi_{uu}(T_c)-1)+3}{(M-1)T_c}\cdot E_s^u}{N_o+\frac{1}{3}\left(\frac{\Delta T}{T_c}\right)^2\sum_{n=0,n\neq u}^{N_u-1}\phi_{un}^2(T_c)\cdot E_s^n}}\right) \tag{58}$$

$$\mathrm{BER}_u^{\mathrm{PSK}}(\Delta T) \approx \frac{2}{m} Q\left(\sqrt{2\sin^2\left(\frac{\pi}{M}\right)\cdot E_s^u\cdot\frac{\frac{\Delta T\left(\frac{\Delta T}{T_c}\phi_{uu}(T_c)+3-\frac{\Delta T}{T_c}\right)(\phi_{uu}(T_c)-1)+3}{3T_c}}{N_o+\frac{1}{3}\left(\frac{\Delta T}{T_c}\right)^2\sum_{n=0,n\neq u}^{N_u-1}\phi_{un}^2(T_c)\cdot E_s^n}}\right) \tag{59}$$

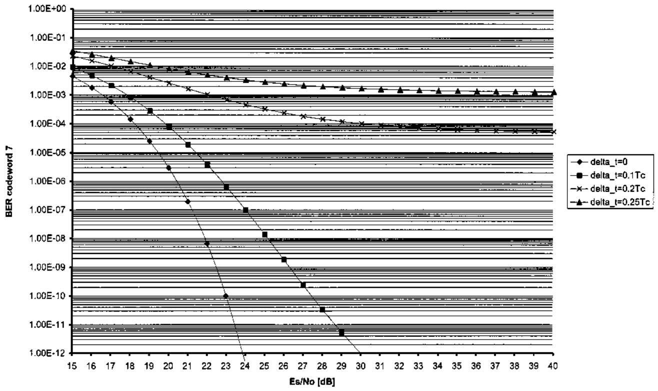

Fig. 10. BER in a QS-CDMA system with codeword 7 out of 8 Walsh–Hadamard codewords and 16-QAM for various timing errors ΔT.

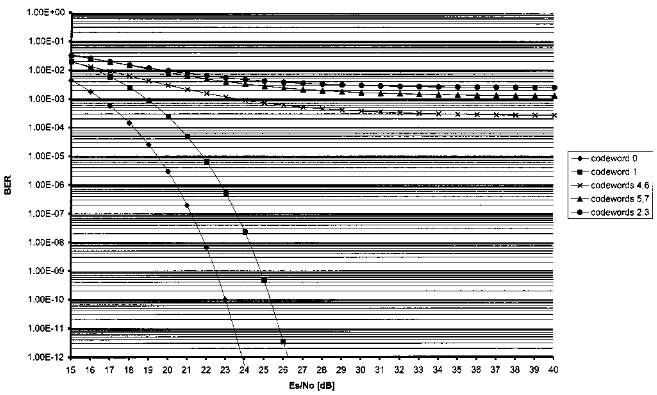

Fig. 11. BER in a QS-CDMA system with 8 Walsh–Hadamard codewords and 16-QAM with a constant timing error of $\Delta T = 0.25T_c$. Results for the different codewords are shown.

Fig. 10 shows the performances of codeword 7 of the code set (note that this codeword has the worst performance). Not all the codewords of the code set have the same performances because their cross corelation and autocorrelation values are different. Fig. 11 shows the performance of the eight different Walsh–Hadamard codewords with 16-QAM and $\Delta T = 0.25T_c$.

C. Comparison Between 16-QAM and 16-PSK with QS-CDMA

This section compares the performances of 16-QAM and 16-PSK used in a QS-CDMA system where the synchronization errors are uniformly distributed. The maximum number of users (length of codeword set) is in this section chosen to be $N = 8$. The BER of QS-CDMA with 16-QAM and 16-PSK for different timing errors is shown in Fig. 12.

From Fig. 12, it can be seen that 16-QAM outperforms 16-PSK for all values of ΔT. From Figs. 8 and 12, it can be seen that 16-QAM with $\Delta T = 0.25T_c$ outperforms QPSK with $\Delta T = 0.5T_c$, so here we can gain something. Hence, QS-CDMA with Walsh–Hadamard codewords and higher-order modulation is interesting if M-QAM is used and not if M-PSK is used.

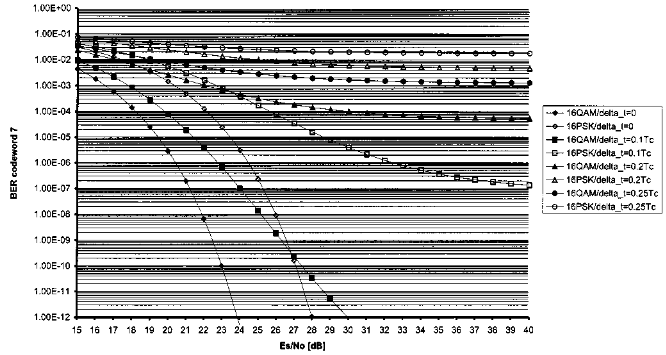

Fig. 12. BER in a QS-CDMA system with 16-QAM and 16-PSK for various timing errors ΔT.

Acknowledgment

The author would like to thank Dr. M. J. M. de Jong for his enthusiastic and professional review of this paper. His contribution was so great that the author considers him the second author of this paper. The author would also acknowledge Prof. K. A. S. Immink for his informative discussions about this subject.

References

[1] J. R. Gibson, Ed., *The Communications Handbook*. Piscataway, NJ: CRC/IEEE press, 1997.

[2] R. de Gaudenzi, C. Elia, and R. Viola, "Band-limited quasi synchronous CDMA: A novel satellite access technique for mobile and personal communication systems," *IEEE J. Select. Areas Commun.*, vol. 10, pp. 328–343, Feb. 1992.

[3] L. R. Welch, "Lower bounds on the maximum cross correlation," *IEEE Trans. Inform. Theory*, vol. IT-20, pp. 397–399, May 1974.

[4] W. R. Braun *et al.*, "Definition of the Mobile Network Synchronization Experiment," Asea Brown Boveri, European Space Agency (ESA-ESTEC), Contract 90/NL/RE, 1990.

[5] V. M. DaSilva and E. S. Sousa, "Multicarrier orthogonal CDMA signals for quasi-synchronous communication systems," *IEEE J. Select. Areas Commun.*, vol. 12, pp. 842–852, June 1994.

[6] H. E. Rowe, "Bounds on the number of signals with restricted cross correlation," *IEEE Trans. Commun.*, vol. COM-30, pp. 966–974, May 1982.

[7] R. de Gaudenzi, "Analysis and performance evaluation of synchronous trellis-coded CDMA for satellite applications," *IEEE Trans. Commun.*, vol. 43, pp. 1400–1408, Feb./Mar./Apr. 1995.

[8] J. M. Wozencraft and I. M. Jacobs, *Principles of Communication Engineering*. Prospect Heights, IL: Waveland Press, 1990.

[9] J. G. Proakis, *Digital Communications*, 2nd ed. New York: McGraw-Hill, 1989.

[10] M. Abramowitz and I. A. Stegun, *Handbook of Mathematical Functions*: National Bureau of Standards, 1964.

[11] W. J. Weber, "Differential encoding for multiple amplitude and phase shift keying systems," *IEEE Trans. Commun.*, vol. COM-26, pp. 385–391, Mar. 1978.

Wim van Houtum (S'93–M'95) was born in Sint-Oedenrode, The Netherlands, in 1964. He received the M.Sc. degree in telecommunication from Eindhoven University of Technology (EUT), Eindhoven, The Netherlands, in 1995.

From 1995 to 1998, he was a Research Scientist at Philips Research Laboratory Eindhoven. He was involved in equalization, modulation, error correction, and access techniques for digital video broadcast systems. Currently, he is a System Architect for wireless networking at Philips Semiconductors Systems Laboratory Eindhoven. His research professional interests include advanced digital modulation techniques and channel-related issues for digital audio/video transmission via satellite, cable, or terrestrial medium.